British Journal of Pharmacology (2004) 142, 1281–1292
www.nature.com/bjp

Intestinal Na^+–K^+–ATPase activity and molecular events downstream of interferon-γ receptor stimulation

[1,2]Fernando Magro, [1]Sónia Fraga, [2]Tomé Ribeiro & *,[1]Patrício Soares-da-Silva

[1]Institute of Pharmacology and Therapeutics, 4200-319 Porto, Portugal and [2]Department of Gastroenterology, Faculty of Medicine, 4200-319 Porto, Portugal

1 This study evaluated the effects of human interferon-γ (IFN-γ) on Na^+–K^+–ATPase activity and the intracellular signaling pathways involved in human intestinal epithelial Caco-2 cells.

2 Na^+–K^+–ATPase activity was determined as the difference between total and ouabain-sensitive ATPase. p38 MAP kinase activity was analyzed by Western blotting using the p38 MAP kinase assay kit. Total and phosphorylated STAT1 protein levels were detected using the PhosphoPlus® Stat1.

3 IFN-γ decreased Na^+–K^+–ATPase activity in a time- and concentration-dependent manner. The IFN-γ-induced decrease in Na^+–K^+–ATPase activity was accompanied by no changes in the abundance of α_1 subunit Na^+–K^+–ATPase. Downregulation of protein kinase C (PKC) with phorbol-12,13-dibutyrate (PDBu) prevented the inhibitory effect of IFN-γ on Na^+–K^+–ATPase activity. Inhibition of Raf-1, mitogen-activated protein kinase kinase (MAPKK/MEK), p38 MAPK and STAT1 with, respectively, GW 5074, PD 98059, SB 203580 and epigallocatechin gallate prevented inhibition of Na^+–K^+–ATPase activity by IFN-γ.

4 Treatment with IFN-γ markedly increased the expression of total and phospho-STAT1, this being accompanied by activation of p38 MAPK. Activation of phospho-STAT1 by IFN-γ was almost abolished by epigallocatechin gallate and markedly reduced by SB 203580, but insensitive to downregulation of PKC.

5 The increase in short circuit current (I_{sc}) by 1.0 and 2.5 $\mu g\,ml^{-1}$ amphotericin B was markedly attenuated in IFN-γ-treated cells. However, the inhibitory effect of PDBu on the amphotericin B-induced increase in I_{sc} was of similar magnitude in vehicle- and IFN-γ-treated cells.

6 It is concluded that IFN-γ markedly attenuates Na^+–K^+–ATPase activity. The transduction mechanisms set into motion by IFN-γ involve the activation of PKC downstream STAT1 phosphorylation and Raf-1, MEK, ERK2 and p38 MAPK pathways, in a complex sequence of events. *British Journal of Pharmacology* (2004) **142,** 1281–1292. doi:10.1038/sj.bjp.0705895

Keywords: Interferon-γ; Na^+–K^+–ATPase; second messengers; Caco-2 cells

Abbreviations: CD, Crohn's disease; EGC, (−)-Epigallocatechin; EGCG, (−)-Epigallocatechin-3-gallate; ERK, extracellular signal-regulated kinases; I_{sc}, short circuit current; IBD, inflammatory bowel disease; IFN-γ, interferon-γ; JAK, Janus kinase; MAPK, mitogen-activated protein kinase; MAPKK, mitogen-activated protein kinase kinase; MEK, MAPK/ERK kinase; PDBu, phorbol-12,13-dibutyrate; PKC, protein kinase C; STAT1, signal transducer and activator transcription factor 1; UC, ulcerative colitis

Introduction

Increasing clinical and experimental data suggest that the induction and pathogenesis of inflammatory bowel disease (IBD), encompassing Crohn's disease (CD) and ulcerative colitis (UC), is a multifactorial process involving interactions among genetic, immune, and environmental factors (Adorini & Francesco, 1997). Indeed, there is substantial evidence to suggest that chronic gut inflammation may arise from a disregulated immune response to components of the normal gut flora. In fact, an imbalance of T helper cell type 1 (Th1) *versus* type 2 (Th2) polarization in favor of Th1 cell subsets appears to be a key pathogenic mechanism in chronic IBD (Adorini & Francesco, 1997). This concept is supported by studies of mucosal biopsies in patients with IBD, demonstrating an increased expression of proinflammatory cytokines, chemokines, and adhesion molecules (Groux & Powrie, 1999). Consistent with the hypothesis of a Th1-mediated pathogenesis in IBD, an increase in interferon-γ (IFN-γ)-secreting cells and IFN-γ mRNA levels, has been described in intestinal lesions of patients with CD (Breese *et al*., 1993; Niessner & Volk, 1995). The importance of Th1-driven immune response in the development of experimental colitis has been also shown. There is also evidence suggesting that TNBS-induced colitis is an IL-12-driven Th1 T cell-mediated colitis and the responding T cells, when stimulated *in vitro*, produce greatly increased amounts of IFN-γ (Neurath *et al*., 1995).

Clinically, the dominant symptom in both CD and UC and 2,4,6-trinitrobenzene sulfonic acid (TNBS) induce colitis is diarrhea, and recent evidence suggests that this may relate to a reduction in electrolyte absorption rather than increases in electrolyte secretion (Sundaram *et al*., 1997). In agreement with this view is the finding that the colonic mucosa of IBD

*Author for correspondence; E-mail: psoaresdasilva@netcabo.pt
Advance online publication: 26 July 2004

patients responds poorly to secretagogues and that Na^+ absorption is diminished (Sandle *et al*., 1990). Consistent with these findings is the observation that IFN-γ reduces agonist-induced and cAMP-induced Cl^- intestinal secretion (Colgan *et al*., 1994). IFN-γ has also been shown to downregulate the cystic fibrosis conductance regulator (CFTR) (Colgan *et al*., 1994), the Na^+–K^+–$2Cl^-$ cotransporter (Zund *et al*., 1996; Fish *et al*., 1999), the Na^+/H^+ exchanger (Rocha *et al*., 2001) and the Na^+–K^+–ATPase (Sugi *et al*., 2001). IFN-γ has direct effects on intestinal epithelial cells, such as changes in cell morphology and decreased levels of proteins involved in transport and barrier function (Madara & Stafford, 1989; Adams *et al*., 1993; Besançon *et al*., 1994; Colgan *et al*., 1994; Fish *et al*., 1999; Sugi *et al*., 2001), but the overall cytoskeletal structure appears to be maintained (Madara & Stafford, 1989). Although the increased production of IFN-γ may have relevant effects on electrolyte and water transport in the inflamed intestine, there is lack of information on the association between IFN-γ and disturbances in intestinal Na^+–K^+–ATPase activity in IBD and experimental colitis. On the other hand, the signaling pathways that initiate the IFN-γ-induced downregulation of electrolyte transporters have not been examined in detail. Some studies suggested that inhibition of Na^+–K^+–ATPase activity by IFN-γ could be mediated by induction of nitric oxide synthase (Unno *et al*., 1995; Sugi *et al*., 2001), but provided no insights on downstream events. However, others have suggested that downregulation of Na^+–K^+–ATPase and ion transporters after prolonged exposure to IFN-γ was unlikely to be mediated by enhanced nitric oxide (Yoo *et al*., 2000).

The signal transduction pathway initiated by binding of IFN-γ to its receptor leads first to Janus kinase (JAK) 1 and 2 activation and their association with the IFN-γ receptor (Haque & Williams, 1998). JAK then phosphorylate IFN-γ receptor on specific tyrosines, which serve as docking sites for the signal transducer and activator transcription factor 1 (STAT1). Recently, IFN-γ was also shown to stimulate mitogen-activated protein kinase (MAPK) activity, namely extracellular signal-regulated kinases (ERK1 and ERK2) (Liu *et al*., 1994) and p38 MAPK (Verma *et al*., 2002). Activation of MAPKs is controlled *via* membrane-associated signaling complexes and involves a network, which includes Ras protein(s), the Raf family (Raf-1, B-Raf, A-Raf, and MEKK) of serine kinases and MAPK kinases, MEK1 and MEK2 as upstream regulators of ERK1 and ERK2 and MEK3 and MEK6 as upstream regulators of p38 MAPK (Pearson *et al*., 2001). STAT1, Raf-1, MEK1, ERK1/2, and p38 MAPK can be probed with specific inhibitors. (−)-Epigallocatechin-3-gallate (EGCG) specifically inhibits the tyrosine phosphorylation of STAT1, but not of STAT3 (Menegazzi *et al*., 2002); (−)-Epigallocatechin (EGC) does not interfere with the tyrosine phosphorylation of STAT1 (Menegazzi *et al*., 2002). GW 5074 is a selective Raf-1 kinase inhibitor (Lackey, 2000). PD 98059 inhibits activation of MAPK/ERK kinase (MEK) and therefore blocks the activation of ERK1/2 (Bobrovskaya *et al*., 2001). p38 MAPK α and β can be inhibited specifically with SB 203580 (Saklatvala *et al*., 1996).

In the present study we have evaluated the effects of IFN-γ on intestinal Na^+–K^+–ATPase activity and the intracellular signaling pathways involved in cultured human intestinal epithelial Caco-2 cells, while using probes that interact Raf-1, MEK, ERK2, p38 MAPK, PKC, and STAT1, and measuring the degree of activation of p38 MAPK and STAT1. It is reported that the decrease in Na^+–K^+–ATPase activity by IFN-γ may involve the activation of PKC downstream STAT1 phosphorylation, and Raf-1, MEK, ERK2, and p38 MAPK pathways in a complex sequence of events.

Methods

Cell culture

Caco-2 cells (ATCC 37-HTB; passages 39–49) were obtained from the American Type Culture Collection (Rockville, MD, U.S.A.) and maintained in a humidified atmosphere of 5% CO_2–95% air at 37°C. Cells were grown in Minimal Essential Medium (Sigma Chemical Company, St Louis, MO, U.S.A.) supplemented with 10^6 U l^{-1} penicillin G, 250 μg l^{-1} amphotericin B, 100 ng l^{-1} streptomycin (Sigma), 20% fetal bovine serum (Sigma), and 25 mmol l^{-1} *N*-2-hydroxyethylpiperazine-*N*′-2-ethanosulfonic acid (HEPES; Sigma). For subculturing, the cells were dissociated with 0.05% trypsin-EDTA, split 1 : 3 and subcultured in Costar Petri dishes with 21 cm^2 growth area (Costar, Badhoevedorp, The Netherlands). For studies on Na^+–K^+–ATPase activity, the cells were seeded in 21 cm^2 plastic culture dishes at a density of 2.0×10^4 cells cm^{-2}. The cell medium was changed every 2 days, and the cells reached confluence after 5 days of initial seeding. For 24 h prior to each experiment, the cell medium was free of fetal bovine serum. Experiments were generally performed 2 days after cells reached confluence, usually 7 days after the initial seeding; each cm^2 contained about 100 μg of cell protein.

Na^+–K^+–ATPase activity

Caco-2 cells cultured in 21 cm^2 plastic culture dishes were dissociated with 0.05% trypsin-EDTA and suspended in Hanks' medium. Na^+–K^+–ATPase activity was measured, under V_{max} experimental conditions, as previously described (Vieira-Coelho *et al*., 2000). Na^+–K^+–ATPase activity is expressed as nanomoles Pi per mg protein per minute and determined as the difference between total and ouabain-sensitive ATPase. The protein content was determined using the DC protein assay kit (Bio-Rad Laboratories, Hercules, CA, U.S.A.) with human serum albumin as a standard.

Na^+–K^+–ATPase immunoblotting

The cells, cultured to 90% confluence, were washed with phosphate-buffered saline (PBS) 2–3 times, lysed by brief sonication (15 s) in PBS, and centrifuged at 20,000 *g* in an Eppendorf table top-refrigerated centrifuge. The pellets were resuspended with ice-cold lysis buffer (10 mM Tris-HCl, pH 8.0, 150 mM NaCl, 1% NP-40, 1 mM PMSF, aprotinin, and leupeptin μg ml^{-1} for NHE3 studies or 10 mM Tris-HCl, pH 8.0, 150 mM NaCl, 1% NP-40, 0.5% Na-deoxycholate, 0.1% SDS, 1 mM PMSF, aprotinin, and leupeptin 10 μg ml^{-1} for Na^+–K^+–ATPase), sonicated briefly, and incubated on ice for 1 h. After centrifugation (Eppendorf table top-refrigerated centrifuge, 14,000 r.p.m. × 30 min), the supernatant was mixed in 6 × sample buffer (0.5 M Tris-HCl, pH 6.8, 7 ml, glycerol 3 ml, SDS 1.04 g, DTT 0.93 g, bromphenol blue 1.2 mg, q.s H_2O to 10 ml) and boiled for 5 min. The proteins were

subjected to SDS–PAGE (8% SDS-polyacrylamide gel) and electrophoretically transferred onto nitrocellulose membranes. The transblot sheets were blocked with 5–10% non-fat dry milk in 25 mM Tris-HCl, pH 7.5, 150 mM NaCl, and 0.1% Tween-20 overnight at 4°C. Then, the membranes were incubated with appropriately diluted antibodies or antisera and the reaction detected by peroxidase-conjugated secondary antibody (Santa Cruz Biotechnology, Santa Cruz, CA, U.S.A.) and ECL system (Amersham Life, Arlington Heights, IL, U.S.A.). Monoclonal antibodies to the purified rabbit α-subunit of Na^+–K^+–ATPase were obtained from Upstate Biotechnology (Lake Placid, NY, U.S.A.). The densities of the appropriate bands were determined using Quantity One (Bio-Rad Laboratories, Hercules, CA, U.S.A.). Protein concentration was measured using the DC protein assay kit (Bio-Rad Laboratories, Hercules, CA, U.S.A.) and bovine serum albumin as standard.

p38 MAP kinase immunoprecipitation and immunoblotting

p38 MAP kinase activity in Caco-2 cells was analyzed by Western blotting using the p38 MAP Kinase assay kit (Cell Signaling Technology™, Beverly, MA, U.S.A.), according to the manufacturer's protocol. Briefly, cells were washed twice with PBS, lysed with cell lysis buffer, and briefly sonicated (15 s). A monoclonal phospho-specific antibody to p38 MAP kinase (Thr180/Tyr182) was used to immunoprecipitate active p38 MAP kinase from cell lysates, overnight at 4°C. Beads were sedimented by centrifugation (1300 r.p.m., 1 min, 4°C) and the pellet was washed with lysis buffer and kinase buffer. The pellet was then suspended in kinase buffer supplemented with 200 μM ATP and 2 μg ATF-2 fusion protein and incubated for 30 min, 30°C. The p38 active MAP kinase ATF-2 induced phosphorylation reaction was terminated by addition of SDS sample buffer (187.5 mM Tris-HCl, pH 6.8, 6% w v^{-1} SDS, 30% glycerol, 150 mM DTT, 0.03% w v^{-1} bromphenol blue). Samples were denatured at 95°C, 5 min and loaded onto 10% SDS–PAGE and electrophoretically transferred onto nitrocellulose membranes. The transblot sheets were blocked for 1 h with 5% of non-fat dry milk in Tris-HCl 25 mM, pH 7.5, NaCl 150 mM, and 0.1% Tween-20, at room temperature. Then, the membranes were incubated with Phospho-ATF-2 (Thr71) antibody (1 : 1000) and the immunocomplexes were detected by the Phototope®-HRP Western detection kit (Cell Signaling Technology™). The densities of the appropriate bands were determined using Quantity One (Bio-Rad Laboratories, Hercules, CA, U.S.A.).

STAT1 immunoblotting

Total and phosphorylated STAT1 protein levels were detected in Caco-2 cells using the PhosphoPlus® Stat1 (Tyr701) antibody kit (Cell Signaling Technology™) according to manufacturer's protocol. Briefly, cells were washed twice with PBS, lysed with SDS sample buffer (62.5 mM Tris-HCl, pH 6.8, 2% w v^{-1} SDS, 10% glycerol, 50 mM DTT, 0.1% w v^{-1} bromphenol blue) and briefly sonicated (15 s). Samples were then denatured for 5 min at 95°C, loaded onto 10% SDS–PAGE, and electrophoretically transferred onto nitrocellulose membranes. The transblot sheets were blocked for 3 h with 5% of non-fat dry milk in Tris-HCl 25 mM, pH 7.5, NaCl 150 mM and 0.1% Tween-20, at room temperature. Then, the membranes were incubated with Phospho-Stat1 or Stat1 antibody (1 : 1000) and the immunocomplexes were detected with the Phototope®-HRP Western detection kit (Cell Signaling Technology™). The densities of the appropriate bands were determined using Quantity One (Bio-Rad Laboratories, Hercules, CA, U.S.A.).

Electrogenic ion transport in Caco-2 cells

Cell monolayers were continuously monitored for changes in short-circuit current (I_{sc}, $\mu A\,cm^{-2}$) after the addition of amphotericin B to the apical-side reservoir, to increase the Na^+ delivered to Na^+–K^+–ATPase to a level approaching saturation (DuVall *et al*., 1998; Vieira-Coelho & Soares-da-Silva, 2001; Gomes & Soares-da-Silva, 2002a, b). Caco-2 cells grown on polycarbonate filters (Snapwell, Costar) were mounted in Ussing chambers (window area 1.0 cm^2) equipped with water-jacketed gas lifts bathed on both sides with 10 ml of Krebs–Hensleit solution, gassed with 95% O_2 and 5% CO_2 and maintained at 37°C. The Krebs–Hensleit solution contained (in mM): NaCl 118, KCl 4.7, $NaHCO_3$ 25, KH_2PO_4 1.2, $CaCl_2$ 2.5, $MgSO_4$ 1.2; pH was adjusted to 7.4 after gassing with 5% CO_2 and 95% O_2. Experimental design also required modification of the bathing solution compositions for specific experiments, and these changes are indicated below. After 5 min stabilization, monolayers were continuously voltage clamped to zero potential differences by application of external current, with compensation for fluid resistance, by means of an automatic voltage current clamp (DVC 1000, World Precision Instruments, Sarasota, FL, U.S.A.). Transepithelial resistance ($\Omega\,cm^2$) was determined by altering the membrane potential stepwise (±3 mV) and applying the Ohmic relationship. Cells were allowed to stabilize for further 25 min before addition of amphotericin B; this period was also used for exposure of cells to the relevant drug treatments. Thereafter, amphotericin B was added to the apical bathing solution to increase the Na^+ delivered to Na^+–K^+–ATPase. Under short-circuit conditions, the resulting current is due to the transport of Na^+ across the basolateral membrane by the Na^+–K^+–ATPase (DuVall *et al*., 1998; Vieira-Coelho & Soares-da-Silva, 2001; Gomes & Soares-da-Silva, 2002a, b). This experimental model allows the entry of apical Na^+ and leads to inhibition of the Na^+/H^+ exchanger (Gomes *et al*., 2001). The effect of ouabain, dibutyril cAMP, phorbol-12,13-dibutyrate (PDBu), 4α-phorbol-12,13-didecanoate (4αPDD) and IFN-γ on amphotericin B-induced increases in I_{sc} was examined in monolayers mounted in Ussing chambers bathed with the standard Krebs–Hensleit solution, such that the final bath Na^+ concentration was 143 mM on both sides of the monolayers. The voltage/current clamp unit was connected to a PC *via* a BIOPAC MP1000 data acquisition system (BIOPAC Systems, Inc., Goleta, CA, U.S.A.). Data analysis was performed using AcqKnowledge 2.0 software (BIOPAC Systems, Inc., Goleta, CA, U.S.A.).

Data analysis

Geometric means are given with 95% confidence limits and arithmetic means are given with s.e.m. Statistical analysis was performed by one-way analysis of variance (ANOVA) followed by Newman–Keuls test for multiple comparisons.

A *P*-value less than 0.05 was assumed to denote a significant difference.

Drugs

Anisomycin, EGCG, EGC, human IFN-γ, human IL-4, human IL-10, human IL-12, human TGF-β, and insulin growth factor I (IGF-I) were obtained from Sigma Chemical Company (St Louis, MO, U.S.A.). GW 5074 (3-(3,5-dibromo-4-hydroxybenzylidene-5-iodo-1,3-dihydro-indol-2-one)) was purchased from Tocris (Tocris Cookson Inc., Avonmouth, U.K.). PD 98059 (2′-amino-3′-methoxyflavone) and SB 203580 (4-(4-Fluorophenyl)-2-(4-methylsulfinylphenyl)-5-(4-pyridyl)1H-imidazole) were obtained from Calbiochem (Calbiochem-Novabiochem Corporation, San Diego, CA, U.S.A.).

Results

To explore the apparent relationship between decreases in sodium epithelial transport and secretion of cytokines involved in inflammation, it was decided to evaluate the effects of proinflammatory (IL-12 and IFN-γ) and anti-inflammatory cytokines (IL-4, IL-10, and TGF-β) on Na^+–K^+–ATPase activity in human intestinal epithelial cells. For that purpose confluent monolayers of Caco-2 cells were used, the cells being treated with human IL-12 (500 U ml^{-1}), IFN-γ (500 U ml^{-1}), IL-4 (500 U ml^{-1}), IL-10 (500 U ml^{-1}), and TGF-β (500 U ml^{-1}). As shown in Figure 1, treatment of Caco-2 cells with human IFN-γ for 24 h, but not IL-12, produced a significant decrease in Na^+–K^+–ATPase activity. On the other hand, treatment of Caco-2 for 24 h with anti-inflammatory cytokines IL-4 and IL-10 did not alter Na^+–K^+–ATPase activity, whereas TGF-β produced a marked increase in sodium pump activity. As growth factors such as the IGF-I have been demonstrated to facilitate intestinal absorption (Gillingham *et al*., 2000), it was decided to evaluate the effect of IGF-I Na^+–K^+–ATPase activity in Caco-2. As shown in Figure 1, IGF-I (500 U ml^{-1}) also increased in sodium pump activity in Caco-2 cells. When cells were treated for 24 h with increasing concentrations of human IFN-γ (100, 300, and 1000 U ml^{-1}), the decrease in Na^+–K^+–ATPase activity was a concentration-dependent effect (Figure 2a). As indicated in Figure 2b, the maximal inhibitory effect of IFN-γ (1000 U ml^{-1}) upon Na^+–K^+–ATPase activity was obtained at 24 h with less marked inhibition at 48 h. Na^+–K^+–ATPase activity in Caco-2 cells was not affected after 1 or 3 h exposure to IFN-γ (1000 U ml^{-1}) (Figure 2b). The IFN-γ-induced decrease in Na^+–K^+–ATPase activity in Caco-2 cells was accompanied by no changes in the abundance of α_1 subunit Na^+–K^+–ATPase (Figure 2c).

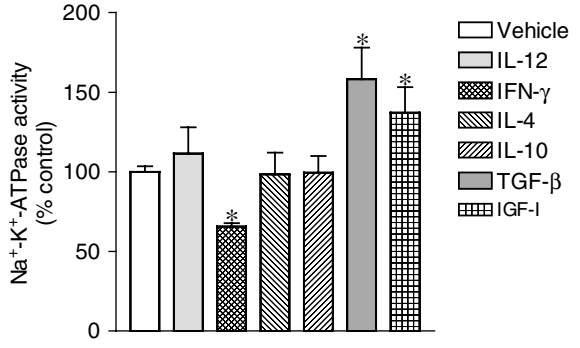

Figure 1 Na^+–K^+–ATPase activity in Caco-2 cells treated for 24 h with vehicle, interleukin-12 (IL-12, 500 U ml^{-1}), interferon-γ (IFN-γ, 500 U ml^{-1}), interleukin-10 (IL-10, 500 U ml^{-1}), interleukin-4 (IL-4, 500 U ml^{-1}), transforming growth factor β (TGF-β, 500 U ml^{-1}) or insulin growth factor I (IGF-I, 500 U ml^{-1}). Enzyme activity is expressed in nanomoles of Pi per mg of protein per min. Columns represent the mean of five experiments per group; vertical lines show s.e.m. Values are percent of control for Na^+–K^+–ATPase activity (absolute levels in nmol Pi per mg protein per min were 44.7 ± 1.2, $n = 5$). *Significantly different from control values ($P < 0.05$) using the Newman–Keuls test.

Physiological assessment experiments of signaling pathways used by IFN-γ were conducted by using a single concentration (1000 U ml^{-1}) and a 24 h exposure of Caco-2 monolayers to human IFN-γ. Cells were pretreated with inhibitors of interest 1 h prior the addition of IFN-γ that was subsequently added to the culture well (inhibitor not washed out). As shown in Figure 3, inhibition of STAT1 and Raf-1 with, respectively, EGCG (Figure 3a) and GW 5074 (Figure 3c) markedly attenuated the inhibitory effect of IFN-γ on Na^+–K^+–ATPase activity. The inactive analog EGC (Figure 3b) did not attenuate the inhibitory effect of IFN-γ upon Na^+–K^+–ATPase activity. From the results shown above one would expect the involvement of MAPK downstream MEK. To test this assumption, cells were treated with PD 98059 (10 μM) and SB 203580 (10 μM). As shown in Figure 3, both PD 98059 (Figure 3d) and SB 203580 (Figure 3e) completely attenuated the inhibitory effect of IFN-γ on Na^+–K^+–ATPase activity. As there is evidence that PKC may function as a serine kinase for STAT1 and an upstream regulator of the p38 MAPK that plays an important role in biological responses to IFN-γ (Watanabe *et al*., 1995), it was decided to test whether PKC is involved in inhibition of Na^+–K^+–ATPase activity by IFN-γ. Treatment of Caco-2 cells with 12,13-dibutyrate (PDBu, 1 μM) resulted in marked inhibition (61.1 ± 5.1% reduction) of Na^+–K^+–ATPase activity. To inhibit the signaling pathway initiated with PKC activation it was decided to downregulate PKC activity. For that purpose, cells were incubated overnight (~18 h) in the presence of phorbol 12,13-dibutyrate (PDBu, 100 nM) (Gomes & Soares-da-Silva, 2002b). As shown in Figure 3f, downregulation of phorbol ester-sensitive PKC isoforms also markedly attenuated the inhibitory effect of IFN-γ on Na^+–K^+–ATPase activity.

STAT1, phospho-STAT1 and phospho-p38 MAPK activation was evaluated in Caco-2 cells exposed to IFN-γ (1000 U ml^{-1}) for 1, 3 and 24 h. Treatment with IFN-γ for 24 h markedly increased total STAT1 and phospho-STAT1 (Figure 4). However, 1 and 3 h treatment with IFN-γ was found to increase phospho-STAT1 only. Treatment with IFN-γ resulted in marked activation of pospho-p38 MAPK, this effect being detected as early as 1 h, persisting over 3 h, and decreasing at 24 h (Figure 4). Activation of phospho-STAT1 after 24 h exposure to IFN-γ (1000 U ml^{-1}) was not affected by EGC (20 μM) (Figure 5b), but significantly attenuated by EGCG (20 μM) (Figure 5d). Activation of phospho-STAT1 after 24 h exposure to IFN-γ (1000 U ml^{-1}) was significantly attenuated by SB 203580 (10 μM) (Figure 6b). On the other hand, downregulation of PKC following overnight exposure of cells to 100 nM PDBu failed to alter the activation of phospho-STAT1 after 24 h exposure to IFN-γ (Figure 6d).

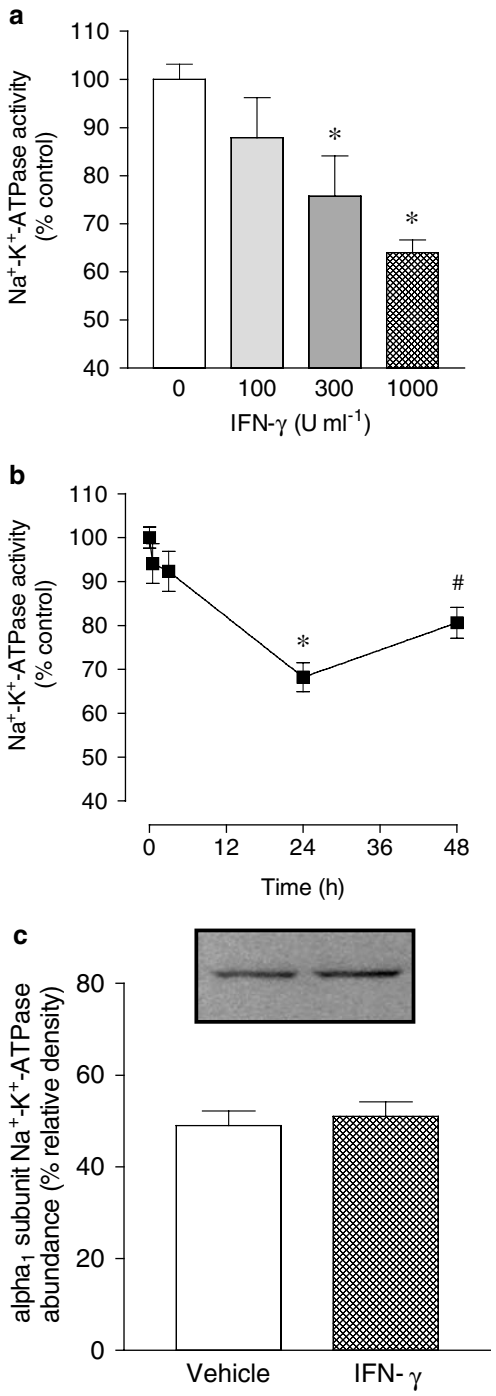

Figure 2 (a) Concentration- and (b) time-dependent effect of interferon-γ (IFN-γ; 1000 U ml^{-1}) on Na^+–K^+–ATPase activity in cultured Caco-2 cells. Columns or symbols represent means of five experiments per group; vertical lines indicate s.e.m. values. Values are percent of control for Na^+–K^+–ATPase activity (absolute levels, in nmol Pi per mg protein per min were 44.7 ± 1.2, $n = 5$). (c) Abundance of α_1 subunit Na^+–K^+–ATPase in membranes of Caco-2 cells treated with vehicle or IFN-γ; 1000 U ml^{-1} for 24 h. Each lane contains equal amounts of protein (20 μg). Columns indicate relative density and represent the mean of four separate experiments; vertical lines indicate s.e.m. Significantly different from control values ($^*P < 0.05$) and values at 24 h ($^{\#}P < 0.05$) using the Newman–Keuls test.

The increase in total STAT1 by IFN-γ (1000 U ml^{-1}) was not affected by EGC (20 μM) (Figure 5a), EGCG (20 μM) (Figure 5c), SB 203580 (10 μM) (Figure 6a) or downregulation of PKC (Figure 6c).

In conditions of 143 mM Na^+ in the extracellular medium, the addition of amphotericin B to the apical cell side induced an increase in I_{sc}, this effect being dependent on the concentration used (Figure 7a). Under these conditions, the amphotericin B-induced increase in I_{sc} was markedly ($P < 0.05$) inhibited by removal of Na^+ from the solution bathing the apical cell border (Figure 7b). Similarly, ouabain (500 μM) markedly reduced the amphotericin B-induced increase in I_{sc} (Figure 7b). Taken together these results suggest that increases in I_{sc} elicited by apical amphotericin B reflect increases in the activity of Na^+–K^+–ATPase located in the basolateral membrane. Previous studies have demonstrated that Na^+–K^+–ATPase is an effector protein for second messenger pathways that include protein kinase A (PKA) and C (PKC) pathways. To evaluate if this was the case in Caco-2 cells using electrophysiological techniques under *in vivo* experimental conditions, the effects of dibutyril cAMP, a direct activator of PKA, and PDBu, a potent activator of PKC, were examined. Treatment of Caco-2 cells for 20 min with dibutyril cAMP (db-cAMP; 500 μM) and PDBu (1 μM) (Figure 7c), applied from both cell sides, effectively reduced the amphotericin B-induced increase in I_{sc}. The inactive phorbol ester 4αPDD (1 μM) was devoid of effect upon changes induced by amphotericin B (data not shown). Incubation of Caco-2 for 20 min with human IFN-γ (1000 U ml^{-1}) failed to reduce the amphotericin B-induced increase in I_{sc}. By contrast, when cells were treated for 24 h with human IFN-γ (1000 U ml^{-1}) the increase in I_{sc} by 1.0 and 2.5 μg ml^{-1} amphotericin B was markedly attenuated (Figure 8a and b). However, the inhibitory effect of PDBu (1 μM) on the amphotericin B-induced increase in I_{sc} was of similar magnitude in vehicle- and IFN-γ-treated Caco-2 cells (Figure 8c). The transepithelial electrical resistance (Ω cm^2) was also identical in vehicle- and IFN-γ-treated Caco-2 cells (90.7 ± 9.6 *versus* 88.5 ± 9.9, $n = 6$).

Discussion

The results presented here show that Na^+–K^+–ATPase activity was markedly reduced by IFN-γ , the effects of which may involve the activation of PKC downstream STAT1 phosphorylation and Raf-1, MEK, ERK2, and p38 MAPK pathways in a complex sequence of events. On the other hand, from the classical counter-regulatory and anti-inflammatory cytokines only TGF-β, but not IL-4 and IL-10, was found to increase Na^+–K^+–ATPase activity in Caco-2 cells. The proinflammatory cytokine IL-12 did not affect Na^+–K^+–ATPase activity in Caco-2 cells. Evidence accumulated over the recent years, however, suggests that IFN-γ is dispensable for the development of TNBS-induced colitis, whereas IL-12 plays a pivotal role in the pathogenesis of experimental colitis (Dohi *et al*., 1999; 2000; Fuss *et al*., 1999; Camoglio *et al*., 2000; Tozawa *et al*., 2003). Though this is evidence suggesting that TNBS-induced colitis is an IL-12-driven Th1 T cell-mediated colitis, it is interesting to observe that Caco-2 cells were insensitive to IL-12 with respect to changes in Na^+–K^+–ATPase activity. This suggests that changes in electrolyte and water transport in the inflamed intestine might result from

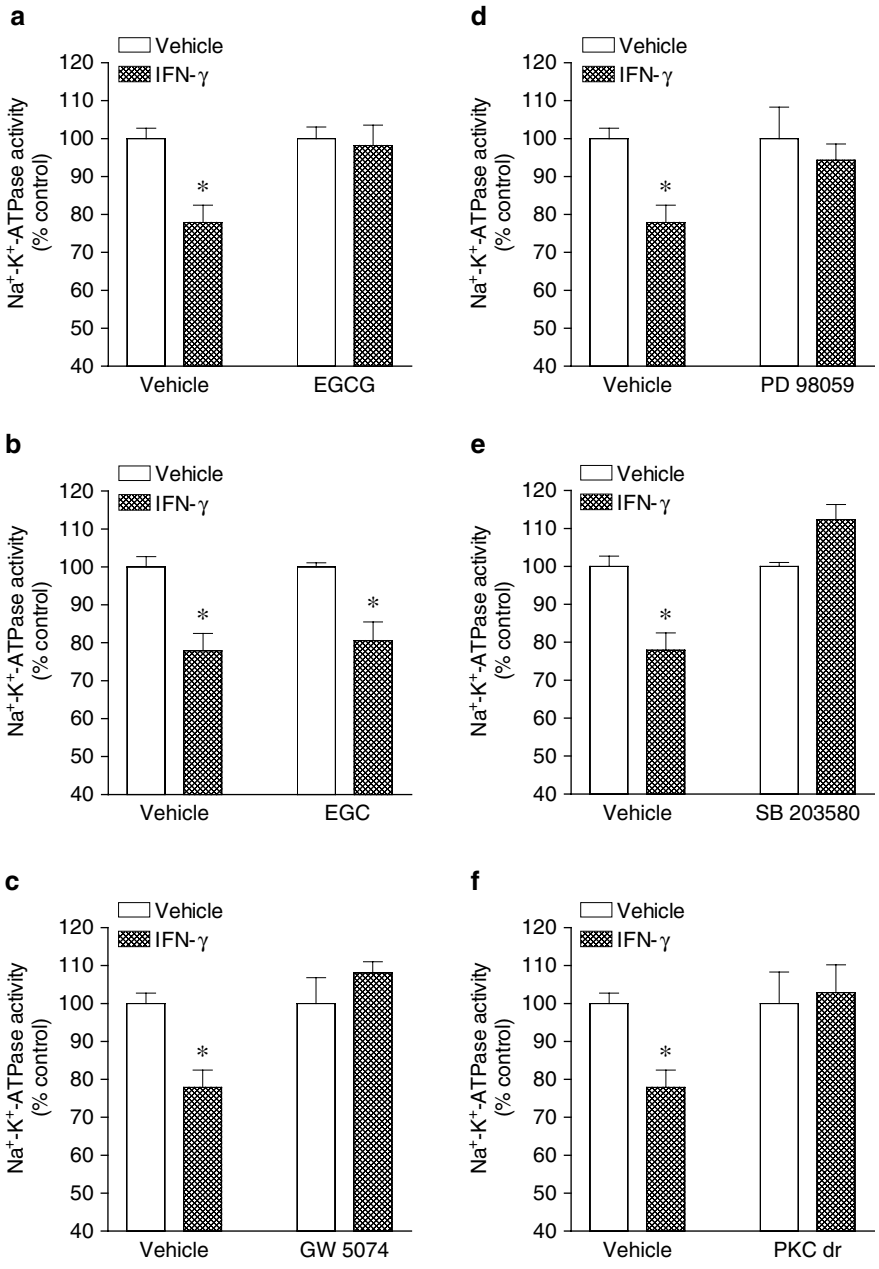

Figure 3 Effect of (a) epigallocatechin-3-gallate (EGCG, 20 μM), (b) epigallocatechin (EGC, 20 μM), (c) GW 5074 (20 nM), (d) PD 98059 (10 μM), (e) SB 203580 (10 μM) and (f) PKC downregulation (PKC dr; overnight treatment with 100 nM PDBu) on human interferon-γ (IFN-γ) induced inhibition of Na^+–K^+–ATPase activity in cultured Caco-2 cells. Columns represent means of five experiments per group; vertical lines indicate s.e.m. values. Values are percent of control for Na^+–K^+–ATPase activity (absolute levels, in nmol Pi per mg protein per min, were 37.7 ± 1.5, $n = 20$). Significantly different from control values ($^*P < 0.05$) using the Student's 't'-test.

IFN-γ-induced decreases in basal Na^+–K^+–ATPase activity and not necessarily from inflammation of the intestinal wall.

As Na^+–K^+–ATPase plays an important role in electrolyte, water and nutrient transport across the intestinal epithelia, it is expected that the IFN-γ-induced decrease in Na^+–K^+–ATPase activity may have a major impact in intestinal function, namely absorption and secretion. This is in agreement with recent data suggesting that IFN-γ-induced down-regulation of ion transport is associated with inhibition of Na^+–K^+–ATPase, which may ultimately result in leaky and dysfunctional epithelium (Yoo *et al*., 2000). The decrease in Na^+–K^+–ATPase activity by IFN-γ in Caco-2 cells was not accompanied by significant decreases in the abundance of the α_1 subunit Na^+–K^+–ATPase. This apparent discrepancy between function and expression of Na^+–K^+–ATPase after IFN-γ is to, a certain extent, in line with that described by others in T84 intestinal cells treated with IFN-γ (Sugi *et al*., 2001). In fact, the IFN-γ-induced decrease in Na^+–K^+–ATPase activity in T84 cells, already observed after 6 h exposure to the cytokine, largely preceded the decrease in Na^+–K^+–ATPase expression, which occurred at 24 h treatment with IFN-γ (Sugi *et al*., 2001). It appears, therefore, that

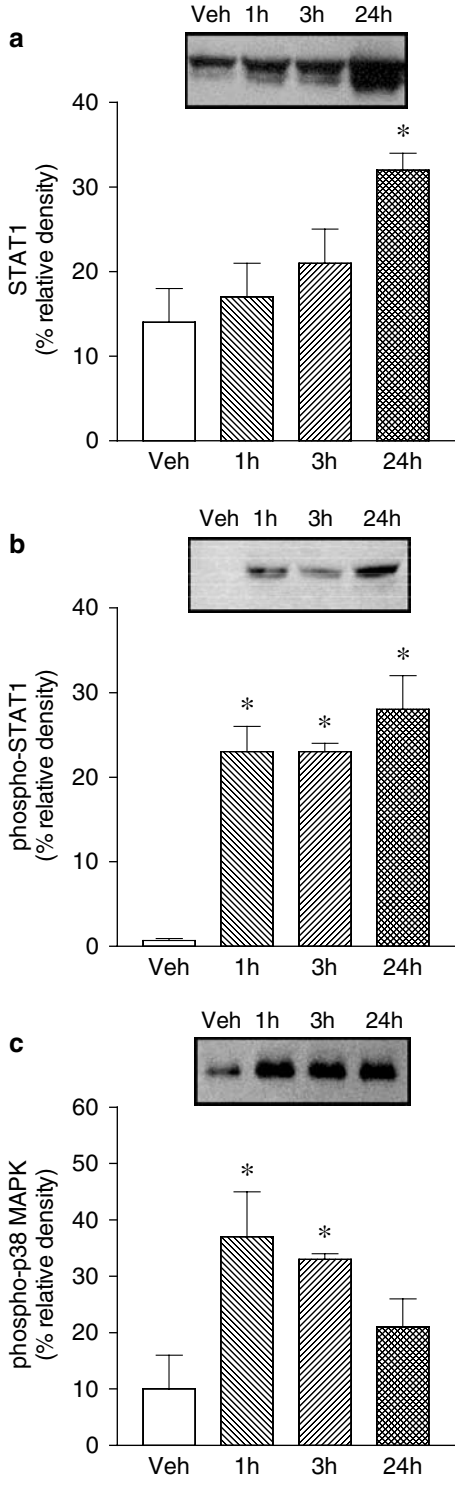

Figure 4 Abundance of (a) total STAT1, (b) phospho-STAT1 and (c) phospho-p38 MAPK in Caco-2 cells treated with vehicle and interferon-γ (IFN-γ, 1000 U ml^{-1}) for 1, 3 and 24 h. Each lane contains equal amount of protein (50 μg). Columns indicate relative density and represent the mean of three to four separate experiments; vertical lines indicate s.e.m. Significantly different from control values (*$P<0.05$) using the Newman–Keuls test.

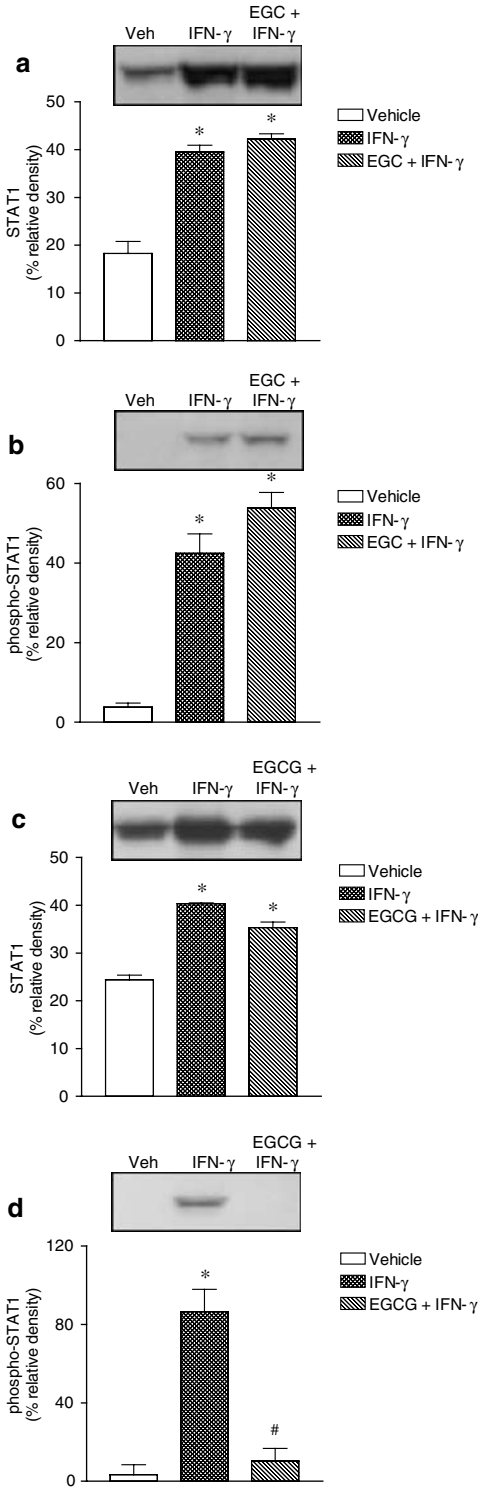

Figure 5 Effect of (a and b) epigallocatechin (EGC, 20 μM) and (c and d) epigallocatechin-3-gallate (EGCG, 20 μM) on the abundance of (a and c) STAT1 and (b and d) phospho-STAT1 in Caco-2 cells treated for 24 h in the absence (vehicle) and in the presence of plus interferon-γ (IFN-γ, 1000 U ml^{-1}). Each lane contains equal amount of protein (50 μg). Columns indicate relative density and represent the mean of three to four separate experiments; vertical lines indicate s.e.m. Significantly different from control values (*$P<0.05$) using the Newman–Keuls test.

there are marked differences between Caco-2 cells and T84 cells concerning the sensitivity of Na^+–K^+–ATPase to IFN-γ. As Na^+–K^+–ATPase activity was measured under V_{max} experimental conditions, using either the biochemical or electrophysiological methods, and the immunoblots concerned total cell protein, the IFN-γ-induced decrease in enzyme

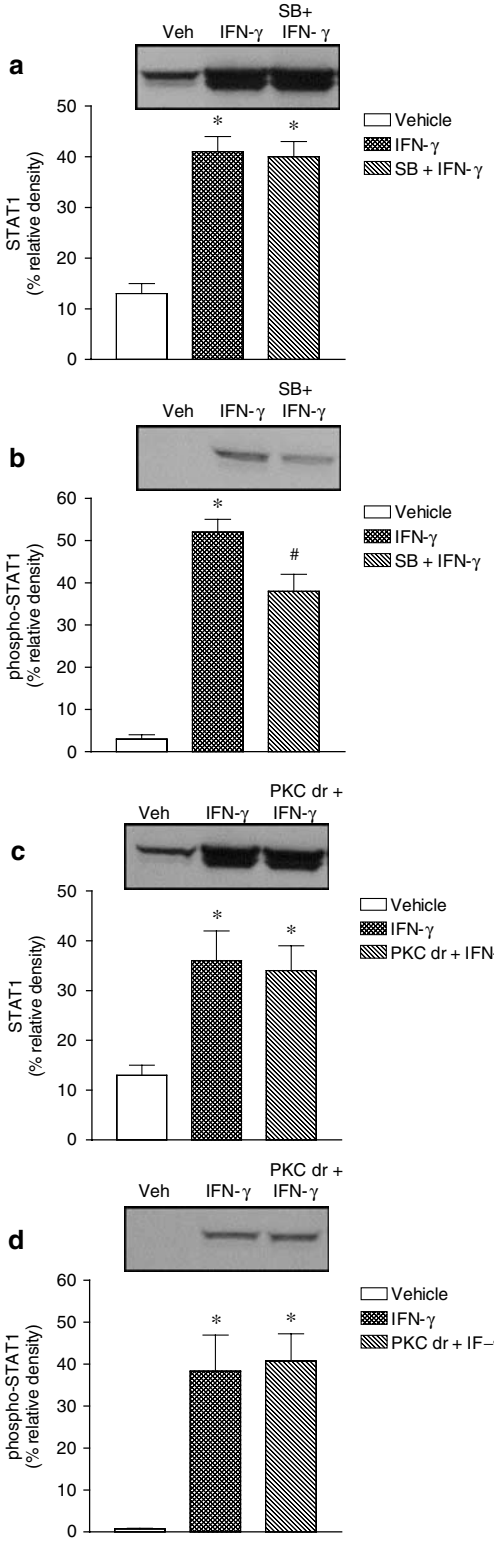

Figure 6 Effect of (a and b) SB 203580 (SB, 10 μM) and (c and d) PKC downregulation (PKC dr; overnight treatment with 100 nM PDBu) on the abundance of (a and c) STAT1 and (b and d) phospho-STAT1 in Caco-2 cells treated for 24 h in the absence (vehicle) and in the presence of plus interferon-γ (IFN-γ, 1000 U ml^{-1}). Each lane contains an equal amount of protein (50 μg). Columns indicate relative density and represent the mean of three to four separate experiments; vertical lines indicate s.e.m. Significantly different from control values (*$P<0.05$) using the Newman–Keuls test.

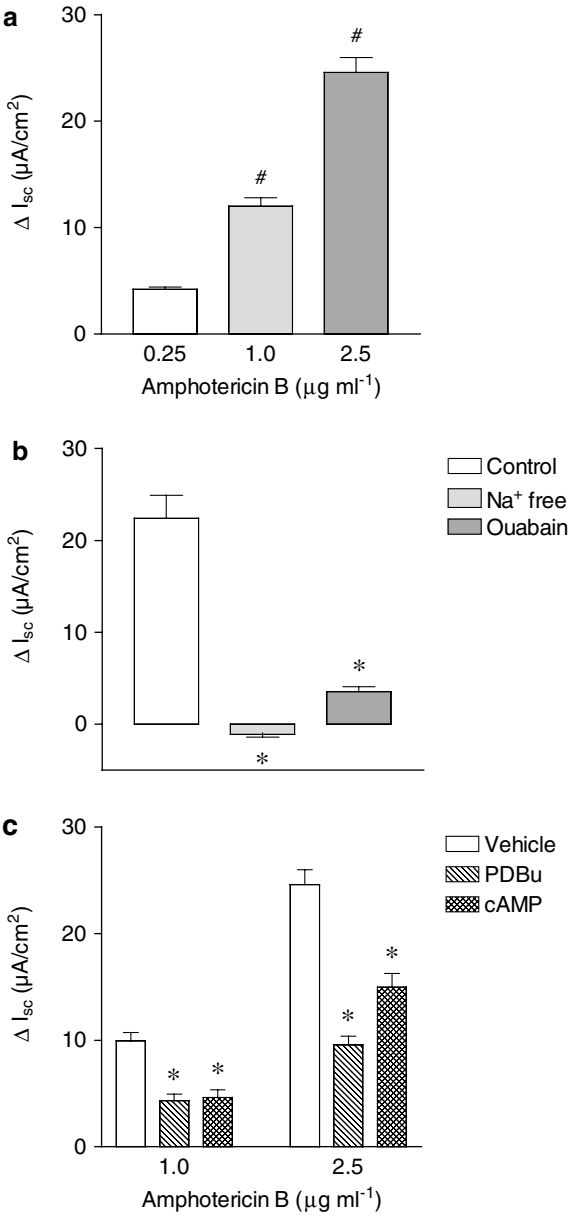

Figure 7 (a) Effect of increasing concentrations of amphotericin B (0.25–2.5 μg ml^{-1}) applied from the apical cell border upon short-circuit current (ΔI_{sc}, μA cm^{-2}) in Caco-2 cells. (b) Effect of removal of Na^+ from the solution bathing the apical cell side and ouabain (500 μM) upon changes in short-circuit current (ΔI_{sc}, μA cm^{-2}) induced by amphotericin B (1.0 μg ml^{-1}) applied from the apical cell side. (c) Effect of cAMP (0.5 mM) and PDBu (1 μM) upon changes in short-circuit current (ΔI_{sc}, μA cm^2) induced by amphotericin B (1.0 and 2.5 μg ml^{-1}) applied from the apical cell side. Columns represent the mean of three to nine experiments per group and vertical lines show s.e.m. Significantly different from values for 0.25 μg ml^{-1} amphotericin B ($^{\#}P<0.05$) or corresponding control values (*$P<0.05$) using the Newman–Keuls test.

activity might reflect a reduction in the number of operational enzyme units in the plasma cell membrane rather than differences in the enzyme affinity for Na^+ or K^+.

Although inhibition of Na^+–K^+–ATPase activity by IFN-γ has been reported before (Guzman *et al*., 1995; Unno *et al*., 1995; Yoo *et al*., 2000; Sugi *et al*., 2001), the signaling

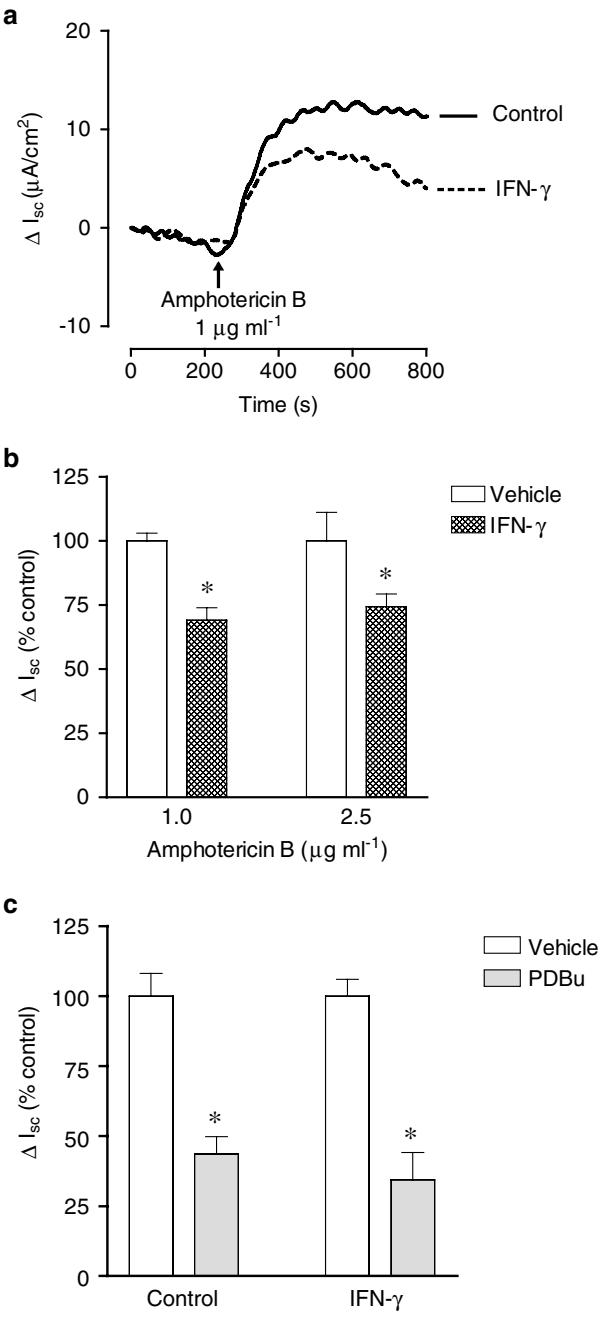

Figure 8 Representative traces (a) and summarized data (b) of the effect of amphotericin B upon short-circuit current (ΔI_{sc}, μA cm^{-2} or ΔI_{sc}, % control) in Caco-2 cells treated for 24 h in the absence (vehicle) and in the presence of plus interferon-γ (IFN-γ, 1000 U ml^{-1}). (c) Effect of PDBu (1 μM) upon changes in short-circuit current (ΔI_{sc}, % control) induced by amphotericin B (1.0 μg ml^{-1}) applied from the apical cell side in Caco-2 cells treated for 24 h in the absence (vehicle) and in the presence of plus interferon-γ (IFN-γ, 1000 U ml^{-1}). Columns represent means of four experiments per group and vertical lines show s.e.m. Significantly different from control values (*$P<0.05$) using the Student's 't'-test.

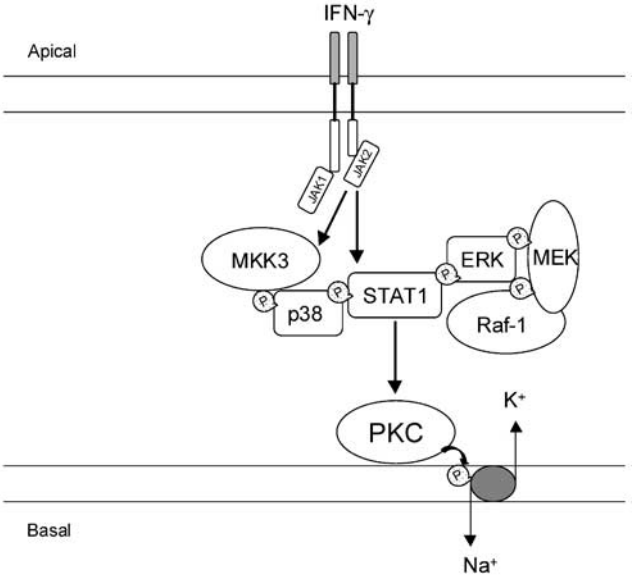

Figure 9 Schematic representation of suggested events downstream IFN-γ receptor activation comprising STAT1 activation with p38 MAPK playing a key role in serine phosphorylation of STAT1. The participation of the Raf/MEK/MAPK cascade might result from STAT1 activation where it functions as a docking protein to permit recruitment of Raf-1. The binding of MEK1 to both Raf-1 and ERK2 and their vicinity with STAT1 might allow these kinases to interact with each other.

pathways that initiate the IFN-γ-induced downregulation of Na$^+$–K$^+$–ATPase have not been examined. Transduction mechanisms set into motion during activation of IFN-γ receptors in Caco-2 cells involve the activation of STAT1, Raf-1, MEK, p38 MAPK and PKC pathways in a complex sequence of events. Though the sequence of events is not entirely apparent from the results of the present studies, some of the findings reported here suggest different types of interactions between the intervening molecular entities. The data presented here strongly suggests that p38 MAPK plays an important role in the regulation of intestinal Na$^+$–K$^+$–ATPase activity. The sensitivity to SB 203580 of IFN-γ-induced inhibition of Na$^+$–K$^+$–ATPase activity strongly suggests that p38 MAPK is involved in the long-term regulation of Na$^+$–K$^+$–ATPase activity. Though preventable by the p38 MAPK inhibitor SB 203580, it is likely that activation of p38 MAPK by IFN-γ may correspond to an event associated with the IFN-γ-induced STAT1 activation. In fact, the STAT1 inhibitor EGCG prevented both the inhibition of Na$^+$–K$^+$–ATPase activity and the increase in phospho-STAT1 expression associated with the long-term exposure to IFN-γ. Though the relationship between p38 MAPK and STAT1 is not apparent from the functional data presented here, it was clearly evidenced that p38 MAPK played a key role in the Ser701 phosphorylation of STAT1 by IFN-γ. In fact, IFN-γ treatment resulted in marked activation of pospho-p38 MAPK and increased expression of phospho-STAT1, this effect being significantly attenuated by SB 203580. IFN-γ was also found to induce STAT1 Ser727 phosphorylation, this being inhibited by SB 203580 (Goh *et al*., 1999). However, other authors have suggested that the interaction between IFN-γ signaling and the p38 MAPK pathway that leads to increased transcriptional activation of STAT1 is independent of Ser727 phosphorylation (Ramsauer *et al*., 2002). On the other hand, evidence demonstrating that the JAK/STAT and Raf/MEK/MAPK signaling cascades are intimately linked (Stancato *et al*., 1997), might explain why the selective Raf-1 kinase inhibitor GW 5074 (Lackey, 2000) and the ERK1/2

inhibitor PD 98059 (Bobrovskaya *et al*., 2001) prevented the inhibitory effect of IFN-γ upon Na^+–K^+–ATPase activity. In addition to its role as a transcription factor, STAT1 may function as a docking protein to permit recruitment of Raf-1 into signaling complexes, containing JAKs, p42 MAP kinase, phosphatidylinositol 3-kinase, and other key regulatory enzymes that modulate both the Raf/MEK/MAPK and JAK/STAT signaling cascades (Stancato *et al*., 1998). More recently, MEKK1 was found to scaffold the ERK2 cascade by binding to each of the three protein kinases of the module, Raf-1, MEK1, and ERK2 (Karandikar *et al*., 2000). The positions of the binding sites on MEKK1 suggest that the three kinases may be closely packed on the MEKK1 surface. As MEK1 binds to both Raf-1 and ERK2 (Fukuda *et al*., 1997), the proximity of their binding sites on MEKK1 might allow these kinases to interact with each other, thereby stabilizing the heteromeric MEKK1 scaffolded complex.

Though the relationship between IFN-γ, Raf/MEK/MAPK cascade, JAK/STAT signaling and PKC is not apparent, several studies have suggested that IFN-γ mediates its cellular effects *via* activation of PKC (Benveniste *et al*., 1991; Lee *et al*., 1995; Lin *et al*., 1996; Flaishon *et al*., 2001; Chang *et al*., 2002). There is evidence that IFN-γ causes a rapid but transient increase in diacylglycerol, the endogenous activator of PKC (Benveniste *et al*., 1991). In addition, the involvement of PKC has also been implicated in the expression of IFN-γ-inducible genes (Benveniste *et al*., 1991). However, the finding that IFN-γ-induced inhibition of Na^+–K^+–ATPase activity in Caco-2 cells is not apparent till 24 h of exposure to the cytokine suggests that the involvement of PKC may be associated with events in the signaling cascade downstream to activation of IFN-γ receptors that leads to Na^+–K^+–ATPase downregulation. This suggestion is supported by the observation that activation of PKC with PDBu in Caco-2 cells leads to marked inhibition of Na^+–K^+–ATPase activity within 30 min. In fact, there is evidence that ERK1/2-dependent IFN-γ-induced activation of STAT1 is partially attenuated by PKC inhibitors (Nguyen *et al*., 2000). In addition, PKC is known to interact with the Raf-1 kinase leading to stimulation of Raf-1 activity (Ueffing *et al*., 1997; Kolch, 2000). On the other hand, the most likely explanation may reside on the activation of PKC downstream STAT1 phosphorylation. This possibility is supported by the observation that downregulation of phorbol ester-sensitive PKC isoforms, following overnight exposure of cells to 100 nM PDBu, failed to reduce the activation of phospho-STAT1 after 24 h exposure to IFN-γ. Taken together, the results presented here strongly suggest that downstream IFN-γ receptor activation to downregulation of Na^+–K^+–ATPase in Caco-2 cells, there is a chain of events (Figure 9) comprising STAT1 activation with p38 MAPK playing a key role in SER701 phosphorylation of STAT1. The binding of MEK1 to both Raf-1 and ERK2 and their vicinity with STAT1 might allow these kinases to interact with each other, which modulates both the Raf/MEK/MAPK and JAK/STAT signaling cascades (Stancato *et al*., 1998).

The majority of studies aimed to evaluate Na^+–K^+–ATPase activity have been performed in broken (i.e., 'unsided') membranes, cell suspensions and isolated intestinal epithelial cells. Using the pore-forming antibiotic amphotericin B to increase the entry of Na^+ through the apical membrane, we were able to isolate Na^+ currents and assess the effects of IFN-γ on the basolateral membrane Na^+–K^+–ATPase activity, in intact Caco-2 cell monolayers. The addition of amphotericin B to the apical cell side increased the Na^+ delivered to Na^+–K^+–ATPase, as indicated by the fast increase in I_{sc}. The transport of Na^+ across the cell monolayer is mediated by Na^+–K^+–ATPase, as indicated by complete prevention by basolateral ouabain and removal of Na^+ from the medium bathing the apical side of the monolayer. Taken together, these results suggest that increases in I_{sc} elicited by apical amphotericin B reflect increases in the activity of Na^+–K^+–ATPase located in the basolateral membrane. The finding that IFN-γ markedly attenuated ouabain-sensitive amphotericin B-induced increases in I_{sc} goes hand-in-hand with the IFN-γ-induced decrease in Na^+–K^+–ATPase activity, as assayed with a biochemical method. Another interesting observation is that IFN-γ did not affect the PDBu-induced inhibition of amphotericin B-induced increases in I_{sc}. This indicates that the PKC-mediated inhibition of Na^+–K^+–ATPase activity is not compromised by the prolonged exposure to IFN-γ, which also decreases Na^+–K^+–ATPase activity in a PKC-dependent manner. On the other hand, the acute effects of PKC activation are not inconsistent with the chronic actions of IFN-γ. In fact, similar PDBu-induced inhibition of Na^+–K^+–ATPase activity in vehicle- and IFN-γ-treated cells differences indicates that chronic exposure to IFN-γ has a minor impact on events related to direct PKC activation. This is likely to be case, namely when considering that 1 μM PDBu is producing maximal inhibition upon Na^+–K^+–ATPase activity; it should be underlined that the magnitude of Na^+–K^+–ATPase activity inhibition by IFN-γ (25% decrease) was approximately half that by acute PDBu (65% decrease).

In conclusion, IFN-γ-mediated inhibition of Na^+–K^+–ATPase activity in human intestinal epithelial Caco-2 cells is evident under *in vitro* and *in vivo* experimental conditions and involves a complex signaling pathway. The transduction mechanisms set into motion by IFN-γ involve the activation of PKC downstream STAT1 phosphorylation and Raf-1, MEK, ERK2 and p38 MAPK pathways in a complex sequence of events.

Supported by Grant POCTI/SAU/14010/98 from *Fundação para a Ciência e a Tecnologia*.

References

ADAMS, R.B., PLANCHON, S.M. & ROCHE, J.K. (1993). IFN-gamma modulation of epithelial barrier function: time course, reversibility, and site of cytokine binding. *J. Immunol.,* **150,** 2356–2363.

ADORINI, L. & FRANCESCO, S. (1997). Pathogenesis and immunotherapy of autoimmune diseases. *Immunol. Today,* **18,** 209–211.

BENVENISTE, E.N., VIDOVIC, M., PANEK, R.B., NORRIS, J.G., REDDY, A.T. & BENOS, D.J. (1991). Interferon-gamma-induced astrocyte class II major histocompatibility complex gene expression is associated with both protein kinase C activation and Na+ entry. *J. Biol. Chem.,* **266,** 18119–18126.

BESANÇON, F., PRZEWLOCKI, G., BARÓ, I., HONGRE, A.S., ESCANDE, D. & EDELMAN, A. (1994). Interferon-gamma downregulates CFTR gene expression in epithelial cells. *Am. J. Physiol. Cell Physiol.,* **267,** C1398–C1404.

BOBROVSKAYA, L., ODELL, A., LEAL, R.B. & DUNKLEY, P.R. (2001). Tyrosine hydroxylase phosphorylation in bovine adrenal chromaffin cells: the role of MAPKs after angiotensin II stimulation. *J. Neurochem.,* **78,** 490–498.

BREESE, E., BRAEGGER, C.P. & CORRIGAN, C.J. (1993). Interleukin-2- and interferon-gamma-secreting T cells in normal and diseased human intestinal mucosa. *Immunol. Today,* **78,** 127–131.

CAMOGLIO, L., TEVELDE, A.A., DE BOER, A., TEN KATE, F.J., KOPF, M. & VAN DEVENTER, S.J. (2000). Hapten-induced colitis associated with maintained Th1 and inflammatory responses in IFN-gamma receptor-deficient mice. *Eur. J. Immunol.,* **30,** 1486–1495.

CHANG, Y.-J., HOLTZMAN, M.J. & CHEN, C.-C. (2002). Interferon-gamma-induced epithelial ICAM-1 expression and monocyte adhesion. Involvement of protein kinase C-dependent c-SRC tyrosine kinase activation pathway. *J. Biol. Chem.,* **277,** 7118–7126.

COLGAN, S.P., PARKOS, C.A., MATTHEWS, J.B., D'ANDREA, L., AWTREY, C.S., LICHTMAN, A.H., DELP-ARCHER, C. & MADARA, J.L. (1994). Interferon-gamma induces a cell surface phenotype switch on T84 intestinal epithelial cells. *Am. J. Physiol. Cell Physiol.,* **267,** C402–C410.

DOHI, T., FUJIHASHI, K., KIYONO, H., ELSON, C.O. & MCGHEE, J.R. (2000). Mice deficient in Th1- and Th2-type cytokines develop distinct forms of hapten-induced colitis. *Gastroenterology,* **119,** 724–733.

DOHI, T., FUJIHASHI, K., RENNERT, P.D., IWATANI, K., KIYONO, H. & MCGHEE, J.R. (1999). Hapten-induced colitis is associated with colonic patch hypertrophy and T helper cell 2-type responses. *J. Exp. Med.,* **189,** 1169–1180.

DUVALL, M.D., GUO, Y. & MATALON, S. (1998). Hydrogen peroxide inhibits cAMP-induced Cl− secretion across colonic epithelial cells. *Am. J. Physiol.,* **275,** C1313–C1322.

FISH, S.M., PROUJANSKY, R. & REENSTRA, W.W. (1999). Synergistic effects of interferon-gamma and tumor necrosis factor alpha on T84 cell function. *Gut,* **45,** 191–198.

FLAISHON, L., LANTNER, F., HERSHKOVIZ, R., LEVO, Y. & SHACHAR, I. (2001). Low levels of IFN-gamma down-regulate the integrin-dependent adhesion of B cells by activating a pathway that interferes with cytoskeleton rearrangement. *J. Biol. Chem.,* **276,** 46701–46706.

FUKUDA, M., GOTOH, Y. & NISHIDA, E. (1997). Interaction of MAP kinase with MAP kinase kinase: its possible role in the control of nucleocytoplasmic transport of MAP kinase. *EMBO J.,* **16,** 1901–1908.

FUSS, I.J., MARTH, T., NEURATH, M.F., PEARLSTEIN, G.R., JAIN, A. & STROBER, W. (1999). Anti-interleukin 12 treatment regulates apoptosis of Th1 T cells in experimental colitis in mice. *Gastroenterology,* **117,** 1078–1088.

GILLINGHAM, M.B., DAHLY, E.M., CAREY, H.V., CLARK, M.D., KRITSCH, K.R. & NEY, D.M. (2000). Differential jejunal and colonic adaptation due to resection and IGF-I in parenterally fed rats. *Am. J. Physiol. Gastrointest. Liver Physiol.,* **278,** G700–G709.

GOH, K.C., HAQUE, S.J. & WILLIAMS, B.R. (1999). p38 MAP kinase is required for STAT1 serine phosphorylation and transcriptional activation induced by interferons. *EMBO J.,* **18,** 5601–5608.

GOMES, P. & SOARES-DA-SILVA, P. (2002a). D_2-like receptor-mediated inhibition of Na^+–K^+–ATPase activity is dependent on the opening of K^+ channels. *Am. J. Physiol. Renal Physiol.,* **283,** F114–F123.

GOMES, P. & SOARES-DA-SILVA, P. (2002b). Role of cAMP-PKA-PLC signaling cascade on dopamine-induced PKC-mediated inhibition of renal Na^+–K^+–ATPase activity. *Am. J. Physiol. Renal Physiol.,* **282,** F1084–F1096.

GOMES, P., VIEIRA-COELHO, M.A. & SOARES-DA-SILVA, P. (2001). Ouabain-insensitive acidification by dopamine in renal OK cells: primary control of the Na^+/H^+ exchanger. *Am. J. Physiol. Regul. Integr. Comp. Physiol.,* **281,** R10–R18.

GROUX, H. & POWRIE, F. (1999). Regulatory T cells and inflammatory bowel disease. *Immunol. Today,* **20,** 442–445.

GUZMAN, N.J., FANG, M.Z., TANG, S.S., INGELFINGER, J.R. & GARG, L.C. (1995). Autocrine inhibition of $Na+/K(+)$-ATPase by nitric oxide in mouse proximal tubule epithelial cells. *J. Clin. Invest.,* **95,** 2083–2088.

HAQUE, S.J. & WILLIAMS, B.R. (1998). Signal transduction in the interferon system. *Semin. Oncol.,* **25,** 14–22.

KARANDIKAR, M., XU, S. & COBB, M.H. (2000). MEKK1 binds Raf-1 and the ERK2 cascade components. *J. Biol. Chem.,* **275,** 40120–40127.

KOLCH, W. (2000). Meaningful relationships: the regulation of the Ras/Raf/MEK/ERK pathway by protein interactions. *Biochem. J.,* **351,** 289–305.

LACKEY, K., CONY, M., DAVIS, R., FAYE, S.V., HARRIS, P.A., HUNTER, R.N., JUNG, D.K., MCDONALD, O.B., MCNUTT, R.W., PEEL, M.R., RUTKOWSKE, R.D., VEAL, J.M., & WOOD, E.R. (2000). The discovery of potent cRaf1 kinase inhibitors. *Bioorg. Med. Chem. Lett.,* **10,** 223–226.

LEE, Y.J., PANEK, R.B., HUSTON, M. & BENVENISTE, E.N. (1995). Role of protein kinase C and tyrosine kinase activity in IFN-gamma-induced expression of the class II MHC gene. *Am. J. Physiol. Cell Physiol.,* **268,** C127–C137.

LIN, H.Y., THACORF, H.R., DAVIS, F.B. & DAVIS, P.J. (1996). Potentiation by thyroxine of interferon-gamma-induced antiviral state requires PKA and PKC activities. *Am. J. Physiol. Cell Physiol.,* **271,** C1256–C1261.

LIU, M.K., BROUWNSEY, R.W. & REINER, N.E. (1994). Gamma interferon induces rapid and coordinate activation of mitogen-activated protein kinase (extracellular signal-regulated kinase) and calcium-independent protein kinase C in human monocytes. *Infect. Immun.,* **62,** 2722–2731.

MADARA, J.L. & STAFFORD, J. (1989). Interferon-gamma directly affects barrier function of cultured intestinal epithelial monolayers. *J. Clin. Invest.,* **83,** 724–727.

MENEGAZZI, M., TEDESCHI, E., DUSSIN, D., PRATI, A.C., CAVALIERI, E., MARIOTTO, S. & SUZUKI, H. (2002). Anti-interferon gamma action of epigallocatechin-3-gallate mediated by specific inhibition of STAT1 activation. *FASEB J.,* **15,** 1309–1311.

NEURATH, M.F., FUSS, I., KELSALL, B.L., STUBER, E. & STROBER, W. (1995). Antibodies to interleukin 12 abrogate established experimental colitis in mice. *J. Exp. Med.,* **182,** 1281–1290.

NGUYEN, V.A., CHEN, J., HONG, F., ISHAC, E.J. & GAO, B. (2000). Interferons activate the p42/44 mitogen-activated protein kinase and JAK-STAT (Janus kinase-signal transducer and activator transcription factor) signalling pathways in hepatocytes: differential regulation by acute ethanol *via* a protein kinase C-dependent mechanism. *Biochem. J.,* **349,** 427–434.

NIESSNER, M. & VOLK, B.A. (1995). Altered Th1/Th2 cytokine profiles in the intestinal mucosa of patients with inflammatory bowel disease as assessed by quantitative reverse transcribed polymerase chain reaction (RT–PCR). *Clin. Exp. Immunol.,* **101,** 428–435.

PEARSON, G., ROBINSON, F., GIBSON, T.B., XU, B.E., KARANDIKAR, M., BERMAN, K. & COBB, M.H. (2001). Mitogen-activated protein (MAP) kinase pathways: regulation and physiological functions. *Endocrine Rev.,* **22,** 153–183.

RAMSAUER, K., SADZAK, I., PORRAS, A., PILZ, A., NEBREDA, A.R., DECKER, T. & KOVARIK, P. (2002). p38 MAPK enhances STAT1-dependent transcription independently of Ser-727 phosphorylation. *Proc. Natl. Acad. Sci. U.S.A.,* **99,** 12859–12864.

ROCHA, F., MUSCH, M.W., LISHANSKIY, L., BOOKSTEIN, C., SUGI, K., XIE, Y. & CHANG, E.B. (2001). IFN-gamma downregulates expression of Na^+/H^+ exchangers NHE2 and NHE3 in rat intestine and human Caco-2/bbe cells. *Am. J. Physiol. Cell Physiol.,* **280,** C1224–C1232.

SAKLATVALA, J., RAWLINSON, L., WALLER, R.J., SARSFIELD, S., LEE, J.C., MORTON, L.F., BARNES, M.J. & FARNDALE, R.W. (1996). Role for p38 mitogen-activated protein kinase in platelet aggregation caused by collagen or a thromboxane analogue. *J. Biol. Chem.,* **271,** 6586–6589.

SANDLE, G.I., HIGGS, N., CROWE, P., MARSH, N.N., VENKATESAN, S. & PETERS, T.J. (1990). Cellular basis for defective electrolyte transport in inflamed human colon. *Gastroenterology,* **99,** 97–105.

STANCATO, L.F., SAKATSUME, M., DAVID, M., DENT, P., DONG, F., PETRICOIN, E.F., KROLEWSKI, J.J., SILVENNOINEN, O., SAHARINEN, P., PIERCE, J., MARSHALL, C.J., STURGILL, T., FINBLOOM, D.S. & LARNER, A.C. (1997). Beta interferon and oncostatin M activate Raf-1 and mitogen-activated protein kinase through a JAK1-dependent pathway. *Mol. Cell. Biol.,* **17,** 3833–3840.

STANCATO, L.F., YU, C.-R., PETRICOIN III, E.F. & LARNER, A.C. (1998). Activation of Raf-1 by interferon and oncostatin M requires expression of the Stat1 transcription factor. *J. Biol. Chem.,* **273,** 18701–18704.

SUGI, K., MUSCH, M.W., FIELD, M. & CHANG, E.B. (2001). Inhibition of Na+,K+-ATPase by interferon gamma down-regulates intestinal epithelial transport and barrier function. *Gastroenterology,* **120,** 1393–1403.

SUNDARAM, U., WISEL, S., RAJENDRAN, V. & WEST, A.B. (1997). Mechanism of inhibition of Na+-glucose cotransport in the chronically inflamed rabbit illeum. *Am. J. Physiol.,* **273,** G913–G919.

TOZAWA, K., HANAI, H., SUGIMOTO, K., BABA, S., SUGIMURA, H., AOSHI, T., UCHIJIMA, M., NAGATA, T. & KOIDE, Y. (2003). Evidence for the critical role of interleukin-12 but not interferon-gamma in the pathogenesis of experimental colitis in mice. *J. Gastroenterol. Hepatol.,* **18,** 578–587.

UEFFING, M., LOVRIC, J., PHILIPP, A., MISCHAK, H. & KOLCH, W. (1997). Protein kinase C-epsilon associates with the Raf-1 kinase and induces the production of growth factors that stimulate Raf-1 activity. *Oncogene,* **15,** 2921–2927.

UNNO, N., MENCONI, M.J., SMITH, M., & FINK, M.P. (1995). Nitric oxide mediates interferon-gamma-induced hyperpermeability in cultured human intestinal epithelial monolayers. *Crit. Care Med.,* **23,** 1170–1176.

VERMA, A., DEB, D.K., SASSANO, A., KAMBHAMPATI, S., WICKREMA, A., UDDIN, S., MOHINDRU, M., VAN BESIEN, K. & PLATANIAS, L.C. (2002). Cutting edge: activation of the p38 mitogen-activated protein kinase signaling pathway mediates cytokine-induced hemopoietic suppression in aplastic anemia. *J. Immunol.,* **168,** 5984–5988.

VIEIRA-COELHO, M.A. & SOARES-DA-SILVA, P. (2001). Comparative study on sodium transport and Na^+,K^+-ATPase activity in Caco-2 and rat jejunal epithelial cells: effects of dopamine. *Life Sci.,* **69,** 1969–1981.

VIEIRA-COELHO, M.A., SERRAO, P., GUIMARAES, J.T., PESTANA, M. & SOARES-DA-SILVA, P. (2000). Concerted action of dopamine on renal and intestinal Na^+–K^+–ATPase in the rat remnant kidney. *Am. J. Physiol. Renal Physiol.,* **279,** F1033–F1044.

WATANABE, I., HORIUCHI, T. & FUJITA, S. (1995). Role of protein kinase C activation in synthesis of complement components C2 and factor B in interferon-gamma-stimulated human fibroblasts, glioblastoma cell line A172 and monocytes. *Biochem. J.,* **305,** 425–431.

YOO, D., LO, W., GOODMAN, S., ALI, W., SEMRAD, C. & FIELD, M. (2000). Interferon-gamma downregulates ion transport in murine small intestine cultured *in vitro*. *Am. J. Physiol. Gastrointest. Liver Physiol.,* **279,** G1323–G1332.

ZUND, G., MADARA, J.L., DZUS, A.L., AWTREY, C.S. & COLGAN, S.P. (1996). Interleukin-4 and interleukin-13 differentially regulate epithelial chloride secretion. *J. Biol. Chem.,* **271,** 7460–7464.

(Received March 9, 2004
Revised May 14, 2004
Accepted June 11, 2004)